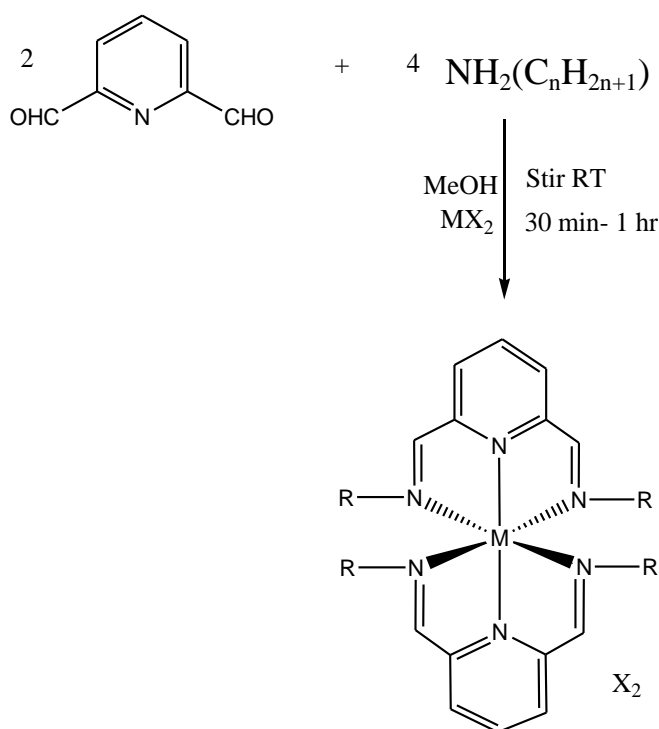


CHAPTER 3 EXPERIMENTAL

3.1 Introduction

This research is focused on first-row transition metal complexes possessing both spin-crossover and metallomesogenic properties. A total of 14 complexes (**Table 3.1** and **3.2**) of general formula $[M(L^n)_2]X_2$, where $M = \text{Co(II)}$, Fe(II) , $L^n =$ Schiff bases formed from the condensation reaction between 2,6-pyridinedicarboxaldehyde and alkylamine of different chain lengths ($n = 6, 8, 10, 12, 14, 16$) and $X = \text{BF}_4$, ClO_4 and PF_6 were prepared and characterized. The general synthetic path is shown in **Scheme 3.1**.



Scheme 3.1 General synthetic path for **Complex 1-14**, R was $\text{C}_n\text{H}_{2n+1}$ and X were BF_4 , ClO_4 and PF_6

Table 3.1 Cobalt(II) complexes

General Formula	<i>n</i>	Complex
$[\text{Co}(L^n)_2](\text{BF}_4)_2$	6	1
	8	2
	10	3
	12	4
	14	5
	16	6
$[\text{Co}(L^n)_2](\text{ClO}_4)_2$	12	7
	16	8
$[\text{Co}(L^n)_2](\text{PF}_6)_2$	6	9

Table 3.2 Iron(II) complexes

General Formula	<i>n</i>	Complex
$[\text{Fe}(L^n)_2](\text{BF}_4)_2$	6	10
	12	11
	16	12
$[\text{Fe}(L^n)_2](\text{ClO}_4)_2$	6	13
$[\text{Fe}(L^n)_2](\text{PF}_6)_2$	6	14

3.2 Chemicals

All chemicals (**Table 3.3**) were commercially available and used as received.

Table 3.3 List of chemicals

Name	Chemical Formula	Formula Weight (g mol ⁻¹)	Supplier
1-Aminodecane	CH ₃ (CH ₂) ₉ NH ₂	157.30	Aldrich
1-Aminododecane	CH ₃ (CH ₂) ₁₁ NH ₂	185.35	Aldrich
1-Aminohexadecane	CH ₃ (CH ₂) ₁₅ NH ₂	241.46	Aldrich
1-Aminohexane	CH ₃ (CH ₂) ₅ NH ₂	101.20	Aldrich
1-Aminooctane	CH ₃ (CH ₂) ₇ NH ₂	129.24	Aldrich
1-Aminotetradecane	CH ₃ (CH ₂) ₁₃ NH ₂	213.40	Aldrich
2,6-Pyridinedicarboxaldehyde	2,6-C ₅ H ₃ N(CHO) ₂	135.12	TCI Europe
Ammonium hexafluorophosphate	(NH ₄)PF ₆	163.00	Aldrich
Cobalt(II) chloride hexahydrate	CoCl ₂ ·6H ₂ O	237.93	Alfa Aesar
Cobalt(II) perchlorate hexahydrate	Co(ClO ₄) ₂ ·6H ₂ O	365.93	Aldrich
Cobalt(II) tetrafluoroborate hexahydrate	Co(BF ₄) ₂ ·6H ₂ O	340.63	Aldrich
Iron(II) chloride tetrahydrate	FeCl ₂ ·4H ₂ O	198.81	Aldrich
Iron(II) tetrafluoroborate hexahydrate	Fe(BF ₄) ₂ ·6H ₂ O	337.55	Aldrich
Iron(II) perchlorate hydrate	Fe(ClO ₄) ₂ ·xH ₂ O	254.75	Aldrich

3.3 Synthesis

The complexes were synthesized by a one-pot reaction.

3.3.1 $[Co(L^6)_2](BF_4)_2 \cdot \frac{1}{2}H_2O$ (Complex 1)

To a magnetically stirred solution of 2,6-pyridinedicarboxaldehyde (0.28 g, 2.10 mmol) in methanol (25 ml) was added dropwise 1-aminohexane (0.41 g, 4.07 mmol), followed by solid $Co(BF_4)_2 \cdot 6H_2O$ (0.35 g, 1.01 mmol) at room temperature. The mixture was stirred for 30 minutes, forming an intensely red brick coloured solution. This solution was concentrated to 5 cm³ on a rotary evaporator, filtered and then washed with diethyl ether. The product was a red brick powder and the yield was 0.74 g (89.1%).

3.3.2 $[Co(L^8)_2](BF_4)_2 \cdot H_2O$ (Complex 2)

The method was the same as in **3.3.1**, using 2,6-pyridinedicarboxaldehyde (0.27 g, 2.01 mmol), 1-aminooctane (0.53 g, 4.08 mmol), and $Co(BF_4)_2 \cdot 6H_2O$ (0.34 g, 1.01 mmol). The product was a red-brick powder and the yield was 0.80 g (82.9%).

3.3.3 $[Co(L^{10})_2](BF_4)_2 \cdot \frac{1}{2}H_2O$ (Complex 3)

The method was the same as in **3.3.1**, using 2,6-pyridinedicarboxaldehyde (0.27 g, 2.01 mmol), 1-aminodecane (0.63 g, 4.02 mmol) and $Co(BF_4)_2 \cdot 6H_2O$ (0.35 g, 1.02 mmol). The product was a red-brick powder and the yield was 0.97 g (91.5%).

3.3.4 $[Co(L^{12})_2](BF_4)_2$ (Complex 4)

The method was the same as in **3.3.1**, using 2,6-pyridinedicarboxaldehyde (0.27 g, 2.01 mmol), 1-aminododecane (0.74 g, 4.02 mmol), and $Co(BF_4)_2 \cdot 6H_2O$ (0.35 g, 1.03 mmol). The product was red brick powder and the yield was 0.89 g (76.2%) after the mixture was directly filtered and washed with diethyl ether. The compound was then recrystallized in methanol:ethanol (1:2) forming red-brick crystals.

3.3.5 [Co(L¹⁴)₂](BF₄)₂.H₂O (Complex 5)

The method was the same as in **3.3.4**, using 2,6-pyridinedicarboxaldehyde (0.27 g, 2.01 mmol), 1-aminotetradecane (0.86 g, 4.01 mmol) and Co(BF₄)₂.6H₂O (0.34 g, 1.01 mmol). The product was a red-brick powder and the yield was 1.16 g (88.8%).

3.3.6 [Co(L¹⁶)₂](BF₄)₂.H₂O (Complex 6)

The method was the same as in **3.3.4**, using 2,6-pyridinedicarboxaldehyde (0.27 g, 2.01 mmol), 1-aminohexadecane (0.97 g, 4.01 mmol) and Co(BF₄)₂.6H₂O (0.34 g, 1.00 mmol). The product was a red-brick powder and the yield was 1.30 g (92.1%).

3.3.7 [Co(L¹²)₂](ClO₄)₂ (Complex 7)

The method was the same as in **3.3.1**, using 2,6-pyridinedicarboxaldehyde (0.27 g, 2.01 mmol), 1-aminododecane (0.74 g, 4.01 mmol) and Co(ClO₄)₂.6H₂O (0.37 g, 1.01 mmol). The product was a red-brick powder and the yield was 0.58 g (48.5%).

3.3.8 [Co(L¹⁶)₂](ClO₄)₂ (Complex 8)

The method was the same as in **3.3.1**, using 2,6-pyridinedicarboxaldehyde (0.27 g, 2.01 mmol), 1-aminohexadecane (0.97 g, 4.02 mmol) and Co(ClO₄)₂.6H₂O (0.37 g, 1.01 mmol). The product was a red-brick powder and the yield was 0.39 g (27.2%).

3.3.9 [Co(L⁶)₂](PF₆)₂ (Complex 9)

Ammonium hexafluorophosphate (0.49 g, 3.01 mmol) was added to CoCl₂.6H₂O (0.24 g, 1.01 mmol) dissolved in 25 ml of methanol. 2,6-Pyridinedicarboxaldehyde (0.27 g, 2.01 mmol) and 1-aminohexane (0.41 g, 4.05 mmol) were added to the solution and stirred at room temperature for one hour. This solution was concentrated to 5 cm³ on a rotary evaporator, filtered and then washed with diethyl ether. The product was a red-brick powder and the yield was 0.75 g (79.1%).

3.3.10 $[Fe(L^6)_2](BF_4)_2$ (Complex 10)

The method was the same as in **3.3.1**, using 2,6-pyridinedicarboxaldehyde (0.27 g, 2.01 mmol), 1-aminohexane (0.41 g, 4.05 mmol), and $Fe(BF_4)_2 \cdot 6H_2O$ (0.34 g, 1.01 mmol). However, intense purple solution was formed when iron(II) salt is added to the solution. The product was a dark purple powder and the yield was 0.69 g (82.7%).

3.3.11 $[Fe(L^{12})_2](BF_4)_2 \cdot H_2O$ (Complex 11)

The method was the same as in **3.3.10**, using 2,6-pyridinedicarboxaldehyde (0.27 g, 2.01 mmol), 1-aminododecane (0.75 g, 4.02 mmol), and $Fe(BF_4)_2 \cdot 6H_2O$ (0.34 g, 1.01 mmol). The product was a dark purple powder and the yield was 0.92 g (78.4%).

3.3.12 $[Fe(L^{16})_2](BF_4)_2$ (Complex 12)

The method was the same as in **3.3.10**, using 2,6-pyridinedicarboxaldehyde (0.28 g, 2.07 mmol), 1-aminohexadecane (0.97 g, 4.05 mmol), and $Fe(BF_4)_2 \cdot 6H_2O$ (0.34 g, 1.01 mmol). The product was a dark purple powder and the yield was 1.30 g (93.2%).

3.3.13 $[Fe(L^6)_2](ClO_4)_2$ (Complex 13)

The method was the same as in **3.3.10**, using 2,6-pyridinedicarboxaldehyde (0.27 g, 2.01 mmol), 1-aminohexane (0.41 g, 4.05 mmol), and $Fe(ClO_4)_2 \cdot 6H_2O$ (0.26 g, 1.02 mmol). The product was a dark purple powder and the yield was 0.45 g (52.1%). It was recrystallized by slow diffusion of diethyl ether forming thick needle like dark purple crystals.

3.3.14 $[Fe(L^6)_2](PF_6)_2$ (Complex 14)

The method was the same as in **3.3.9**, using ammonium hexafluorophosphate (0.49 g, 3.01 mmol), $FeCl_2 \cdot 4H_2O$ (0.21 g, 1.06 mmol), 2,6-pyridinedicarboxaldehyde (0.27 g, 2.01 mmol) and 1-aminohexane (0.41 g, 4.05 mmol). The product was a dark purple powder and the yield was 0.80 g (84.7%).

3.4 Instrumental Analyses

The complexes were characterized by elemental microanalyser, electrospray ionization-mass spectrometer (ESI-MS), and fourier transform infrared (FTIR) and UV-Visible spectroscopies. Their thermal properties were determined by thermogravimetry (TGA), differential scanning calorimetry (DSC) and polarizing optical microscopy (POM), while the magnetic properties were determine using the Guoy balance and SQUID magnetometer. The analyses were done using facilities in University of Leeds, United Kingdom and at the Chemistry Department, Science Faculty, University of Malaya.

3.4.1 Elemental analyses

Elemental microanalyses were performed by the School of Chemistry microanalytical service, University of Leeds or using a Perkin-Elmer CHNS/O analyser 2400 Series II at University of Malaya. A small amount of sample (1 – 2 mg) was placed in a tin capsule with the dimension of 5 x 8 mm and was folded into tiny piece. It was then put into the analyser and heated up to 1000 °C.

3.4.2 Electrospray ionization mass spectroscopy

The ESI-MS were done on a Bruker Daltonics (microTOF) at the School of Chemistry, Leeds University. A very small amount of samples were dissolved in methanol, and the solution injected to the receiver.

3.4.3 Fourier transform infrared spectroscopy

The FTIR spectra were recorded as nujol mulls pressed between NaCl windows between 450-4000 cm^{-1} , using a Nicolet Avatar 360 spectrophotometer at the University of Leeds, while FTIR spectrum were recorded on neat samples using Perkin-Elmer Spectrum 400 FT-IR/FT-IR Spectrometer with a Pike 22107 Technologies GladiATR attachment at University of Malaya.

3.4.4 UV-vis spectroscopy

The UV-vis spectra were recorded between 1200-400 nm on a Shimadzu UV-vis-NIR 3600 spectrophotometer. Each sample was dissolved in suitable solvent (chloroform) in a 10-ml volumetric flask. The solution was placed into a 1-cm quartz cuvette and inserted into the spectrometer holder. The data was collected against the solvent as background.

3.4.5 X-ray crystallography

The single crystal X-ray diffraction data was collected from either a Bruker Apex II CCD diffractometer at 100 K employing graphite-monochromated Mo-K α radiation or a Bruker X8 Apex diffractometer using graphite-monochromated Mo-K α radiation ($\lambda = 0.71073 \text{ \AA}$) generated by a rotating anode. The structures were solved by direct method using SHELXS-97 and refined by full matrix least square methods on F².

3.4.6 Room-temperature magnetic susceptibility

Room-temperature magnetic susceptibility was carried out using Guoy method. A finely ground sample was placed into the glass tube to a height of 2-3 cm (exactly known) before it was introduced into the balance. The $R-R_0$ value was recorded. The value of χ_g can be calculated using the following equation:-

$$\chi_g = \frac{C_{bal} l (R - R_0)}{10^9 m}$$

where, C_{bal} = balance calibration constant, l = length of the sample in tube (cm), R = reading of empty tube, R_0 = reading of tube with l of sample, m = mass of sample in tube (g).

For some samples, the χ_g values were measured using Sherwood Auto Magnetic Susceptibility balance. Finely ground sample was packed into the tube at 2 cm length before placing it inside the balance. χ_g value was recorded directly from the reading on

the instrument. From the relationship shown below, mass magnetic susceptibility (χ_m) and the effective magnetic moment (μ_{eff}) of the sample can be calculated.

$$\chi_M = \chi_g (\text{Formula weight in g mol}^{-1})$$

$$\mu_{\text{eff}} = 2.84(\chi_M^{\text{corr}} T)^{1/2}$$

where T = absolute temperature in (K) and χ_M^{corr} is the molar susceptibility corrected for the diamagnetic components of the ligands and associated ions (*see appendices*).

3.4.7 Variable-temperature magnetic susceptibility

Variable-temperature magnetic susceptibility measurements were performed using Quantum Design Superconducting Quantum Interference Device (SQUID) magnetometer in an applied field of 1000 or 5000 G in the temperature range 400-4 K at University of Manchester, UK.

3.4.8 Variable-temperature UV-visible

Similar to room-temperature UV-visible, the UV-vis spectra were recorded between 900-400 nm on a Shimadzu UV-vis-NIR 3600 spectrophotometer in temperature range from 5 °C to 70 °C in 5 °C interval.

3.4.9 Thermogravimetry

The TGA traces were recorded on a TA Instrument model Q50 V20.13 Build 39, heating from 25-500 °C at Leeds University or on a Perkin-Elmer Pyris Diamond TG/DTA thermal instrument at University of Malaya. The thermographs were recorded in the temperature range 50-900 °C under N₂ at a flow rate of 10 cm³ min⁻¹ and a scan rate of 20 °C min⁻¹.

3.4.10 Differential scanning calorimetry

DSC were performed using a Mettler Toledo model DSC 822E. Two heating and cooling cycles were recorded with the scan rate between 5-10 °C min⁻¹ depending on

suitability of the samples and in the range 25 – 200 °C under N₂ at a flow rate of 20 cm³ min⁻¹. The onset temperatures were quoted for all peaks observed.

3.4.11 Polarizing optical microscopy

The photomicrographs were viewed under Nikon-H600L Eclipse Microscopes, both equipped with a Mettler Toledo FP90 central processor and a Linkam THMS 600 hot stage, and the magnification was 50x. Small amount of a sample was sandwiched between two glass slides and then placed onto the hot stage. The temperature of the hot stage was set 10-20°C below the decomposition temperature of each sample. Heating and cooling rates can be adjusted between 2-5 °C min⁻¹ or 10 °C min⁻¹ depending on the suitability of the samples.